Supplementary Online Content

Byun MS, Park SW, Lee JH, et al; KBASE Research Group. Association of retinal changes with Alzheimer disease neuroimaging biomarkers in cognitively normal individuals. *JAMA Ophthalmol*. Published online March 25, 2021. doi:10.1001/jamaophthalmol.2021.0320

This supplementary material has been provided by the authors to give readers additional information about their work.

eMethods. Detailed Methods

Recruitment of participants and clinical assessment

For the present study, cognitively normal (CN) older adults were recruited from the cohort of Korean Brain Aging Study for Early Diagnosis and Prediction of Alzheimer's Disease (KBASE), an ongoing prospective cohort study started in 2014. Details of the KBASE cohort are described in our previous report.[1] Briefly, inclusion criteria of the CN older adults in the KBASE cohort study were as follows: a) age range of 55 – 90 years (inclusive); b) a global Clinical Dementia Rating score of 0; and c) without diagnosis of MCI or dementia. Exclusion criteria of KBASE cohort study were: a) Presence of major psychiatric illness, significant neurological or medical condition or comorbidities that could affect mental function; b) contraindications for MRI scan; c) illiteracy; d) presence of significant visual/hearing difficulty; severe communication or behavioral problems that interfere with ease of performance of clinical examination or brain scan difficult; e) receiving investigational drug treatment; and f) pregnant or breastfeeding. All participants completed clinical and neuropsychological assessments, [^{11}C] PiB-PET and MRI scan, and blood sampling. In all subjects, standardized clinical and neuropsychological assessments were performed by trained psychiatrists and neuropsychologists based on the KBASE clinical and neuropsychological assessment protocol which incorporated the Korean version of the Consortium to Establish a Registry for Alzheimer`s Disease Assessment Packet (CERAD-K)[2] and the CERAD-K neuropsychological battery.[3] In addition, vascular risk factors such as hypertension, diabetes mellitus, coronary heart disease, and hyperlipidemia were assessed by a systematic interview with participants and their informants by trained nurses.[1] Apolipoprotein E (APOE) genotyping was conducted using DNA extracted from whole blood[4] and the presence of at least one ε4 allele was considered as APOE ε4 carrier (APOE4).

Initially, a total of 59 CN older adults from the KBASE cohort were recruited for this study. After ophthalmic examination, participants with presence of significant ophthalmic condition that affects vision (*e.g.*, glaucoma, severe myopia, severe cataract, retinal vascular occlusion, and epiretinal membrane) were excluded for final analysis. Four subjects who had unpredicted retinal disease (i.e., epiretinal membrane) were excluded and another six subjects were excluded due to data missing or unavailability. Thus, a total of 49 participants were included for final analysis.

Image acquisition and pre-processing

All participants underwent simultaneous three-dimensional (3D) [^{11}C] PiB-PET and 3D T1-weighted MRI using the 3.0T Biograph mMR (PET-MR) scanner (Siemens, Erlangen, Germany). Details of acquisition of [^{11}C] PiB-PET and MRI are described in the previous studies.[5] In brief, Statistical Parametric Mapping 8 (SPM8; http://www.fil.ion.ucl.ac.uk/spm) was used for image preprocessing of [^{11}C] PiB-PET. After co-registered static PiB-PET images to individual T1 structural images, transformation parameters of individual T1 images to a standard Montreal Neurological Institute (MNI) template were calculated for the spatial normalization. Subsequently, we used the inverse transformation parameters to transform coordinates from the automatic anatomic labeling (AAL) 116 atlas [6] to an individual space for each subject (resampling voxel size = 1 × 0.98 × 0.98 mm) using IBASPM software, and the non-gray matter (GM) portions of the atlas were excluded by using the image of cerebral GM segment.

For measurement of cerebral Aβ deposition, regions of interests (ROIs), including the frontal, lateral parietal, posterior cingulate-precuneus, and lateral temporal regions were first determined by applying the automatic anatomic labeling algorithm and region combining method.[7] Subsequently, we calculated the standardized uptake value ratio (SUVR) values for each ROI by dividing the mean [^{11}C]-PiB uptake value for all voxels within each ROI were calculated by the mean cerebellar GM [^{11}C]-PiB uptake value.

In this study, dichotomized Aβ variable rather than continuous variable was used because of characteristics of disproportionate distribution of global Aβ deposition in cognitively normal (CN) population as described in previous reports,[8,9] as well as in our data which showed a non-normal distribution of global [^{11}C]-PiB retention value as demonstrated in e-Figure1. The present study adopted the regional definition of PiB positivity with 1.4 cutoff value to more sensitively detect CN older adults with increased Aβ burden based on a number of previous literatures including those from our group.[5,7,10-15] Thus, CN older adults were classified as either the Aβ positive group (Aβ+CN) if the standardized uptake value ratio (SUVR) was > 1.4 in at least one of the four regions of interests (ROIs) including the frontal, lateral parietal, posterior cingulate-precuneus, and lateral temporal regions, where Aβ mainly accumulates in early AD[16], or as the Aβ negative group (Aβ-CN) if the SUVR of all four ROIs was ≤ 1.4.[7,10,14]

Evaluation of the retina using swept source-optical coherent tomography (SS-OCT) and multifocal electroretinography (mfERG)

Macular thickness was measured using SS-OCT (DRI-OCT-1 Atlantis; Topcon, Tokyo, Japan).In all participants, the 3D raster scan modality of SS-OCT was applied by trained examiners after dilation of the pupil. Using this scan protocol, a retinal and choroidal tomography map is obtained with 512 horizontal and 256 vertical A-scans, which allows mapping of the retinal and choroidal thickness of the entire macular area (12 × 9 mm) after automated segmentation of the retinal layers including the choroid. The SS-OCT scans were analyzed to verify location of the reference at the inner and outer boundary of the retina and choroid through automated delineation. Retinal thickness map was overlapped with a 6 × 6 mm grid of the Early Treatment Diabetic Retinopathy Study (ETDRS) to assess the different mean values of each sector. The mean thickness of each sector was automatically measured at ≤ 500 μm distance from the center of the fovea in the central sector, ≤ 500 – 1500 μm distance from that in the parafoveal sectors (nasal, inferior, temporal, and superior), and ≤ 1500 – 3000 μm from that in four perifoveal sectors (nasal, inferior, temporal, and superior). After obtaining the macular thickness at nine ETDRS areas, the average macular thickness in the central fovea, inner ring (parafovea), and outer ring (perifovea) was calculated and used for analysis.

Thickness of the GCIPL and RNFL were measured using the same SS-OCT and procedure as that used for macular thickness. With the built-in analysis software (version 9.30; Topcon, Tokyo, Japan), the RNFL boundary was automatically segmented and the RNFL thickness throughout the scan was calculated. An RNFL thickness map was generated within a 12 × 9-mm field area with color scales corresponding to the numeric values of RNFL thickness. In addition, a macular GCIPL thickness map within 6.0 × 6.0-mm^2 macular area was generated.

The mfERG (RETI-scan; Roland Consult, Stasche & Finger GmbH, Wiesbaden, Germany) was recorded using ERG-Jet electrodes, according to the ISCEV guideline for clinical multifocal electroretinography.[17] Patients' fixation was continuously monitored using a camera system. Two recordings were obtained of approximately 4 minutes' duration each. Any large eye movements or fixation losses were rejected, and the recording was repeated. The retinal area stimulated by the central hexagon was ring 1 between 0 and 1.7°, ring 2 between 1.7 and 5.6°, ring 3 between 5.6 and 10.2°, ring 4 between 10.2 and 15.6°, ring 5 between 15.6 and 21.7°, and ring 6 between 21.7 and 28.6° eccentricity from the fovea on either side. Both trace array and ring presentation of first-order kernels were performed and evaluated. A single iteration of artifact rejection was applied to the raw data, whereas no spatial smoothing was applied before derivation of the first- and second-order kernels, implicit times, and amplitudes of the mfERG components N1 (first negative), P1 (first positive), and N2 (second negative). The N1 response amplitude was measured from the starting baseline to the base of the N1 trough, the P1 response amplitude was measured from the N1 trough to the P1 peak, and the N2 response amplitude was measured from the P1 peak to the N2 trough.

Receiver operating characteristic (ROC) curve analyses

After selection of final model using the backward likelihood ratio (LR) from the logistic regression analyses with Aβ positivity as an outcome variable, a logistic regression analyses with only fixed variables (i.e., age, sex, APOE4, and best-corrected visual acuity) was conducted as a reference model. Then, the receiver operating characteristic (ROC) curve analyses was performed using the fitted values derived from these models and area under the curve (AUC) of ROC curves were compared by using the method of Delong.[18]

eTable 1. Comparison of macular thickness of retina between the Aβ–CN and Aβ+CN groups.

Macular thickness	Aβ–CN (N = 33)	Aβ+CN (N = 16)	*P*
Central fovea	234.5 ± 22.9	227.7 ± 25.4	.76
Inner ring average (Parafovea)	305.3 ± 17.0	286.3 ± 18.8	.02
Outer ring average (Perifovea)	268.4 ± 16.0	258.5 ± 10.7	.37

NOTE. Data are presented as mean ± SD. The unit of all parameters is μm. Covariates including age, sex, *APOE4* carrier status and visual acuity were adjusted.

Abbreviations: Aβ, amyloid-β; CN, cognitively normal; Aβ+CN, amyloid positive CN; Aβ-CN, amyloid negative CN

eTable 2. Subregional comparison of the thickness of the inner ring of the macula between the Aβ–CN and Aβ+CN groups.

Thickness of the sub-regions of inner ring of the macula	Aβ–CN (N = 33)	Aβ+CN (N = 16)	*P*
Inner superior	306.6 ± 18.6	288.4 ± 20.6	.06
Inner temporal	299.1 ± 16.5	282.1 ± 17.0	.06
Inner inferior	306.5 ± 17.1	288.7 ± 21.4	.04
Inner nasal	308.9 ± 18.4	286.1 ± 22.5	.007

NOTE. Data are presented as mean ± SD. The unit of all parameters is μm. Covariates including age, sex, *APOE4* carrier status and visual acuity were adjusted.

Abbreviations: Aβ, amyloid-β; CN, cognitively normal; Aβ+CN, amyloid positive CN; Aβ-CN, amyloid negative CN

eTable 3. Comparison of retinal layer thickness between the Aβ–CN and Aβ+CN groups.

Parameters	Aβ–CN (N = 33)	Aβ+CN (N = 16)	*P*
Average RNFL thickness	104.8 ± 10.6	86.0 ± 31.5	.006
Average GCIPL thickness	69.2 ± 7.4	64.4 ± 6.7	.4

NOTE. Data are presented as mean ± SD. The unit of all parameters is μm. Covariates including age, sex, *APOE4* carrier status and visual acuity were adjusted.

Abbreviations: Aβ, amyloid-β; CN, cognitively normal; Aβ+CN, amyloid positive CN; Aβ-CN, amyloid negative CN

eTable 4. Subregional comparison of the thickness of the RNFL quadrants between the Aβ–CN and Aβ+CN groups.

Thickness of the RNFL quadrants	Aβ–CN (N = 33)	Aβ+CN (N = 16)	*P*
Superior	127.5 ± 18.4	104.2 ± 51.1	.04
Temporal	81.0 ± 12.1	63.9 ± 26.0	.007
Inferior	133.8 ± 17.9	103.8 ± 43.5	.003
Nasal	76.1 ± 13.6	71.4 ± 26.6	.36

NOTE. Data are presented as mean ± SD. The unit of all parameters is μm. Covariates including age, sex, *APOE4* carrier status and visual acuity were adjusted.

Abbreviations: Aβ, amyloid-β; CN, cognitively normal; Aβ+CN, amyloid positive CN; Aβ-CN, amyloid negative CN

eTable 5. Comparison of functional parameters of retina measured by mfERG between the Aβ–CN and Aβ+CN groups.

	Amplitude (nV/deg^2)			Implicit time (ms)		
	Aβ–CN (N = 33)	**Aβ+CN (N = 16)**	***P***	**Aβ–CN (N = 33)**	**Aβ+CN (N = 16)**	***P***
Ring 1	93.8 ± 31.7	91.4 ± 42.1	.66	41.1 ± 5.8	42.7 ± 6.2	.28
Ring 2	59.7 ± 15.7	55.9 ± 23.5	.997	39.3 ± 1.6	40.8 ± 3.7	.04
Ring 3	40.8 ± 10.7	45.3 ± 14.0	.17	38.1 ± 1.1	40.2 ± 3.2	.003
Ring 4	29 ± 8	28.2 ± 9.1	.53	37.9 ± 1.3	39.6 ± 3.3	.009
Ring 5	21.5 ± 5.6	22 ± 7.6	.42	38.2 ± 1.3	41.3 ± 4	.002
Ring 6	14.7 ± 4.1	15.6 ± 6.3	.25	39.2 ± 1.7	42 ± 4.2	.02

Note. Data are presented as mean ± SD. Covariates including age, sex, *APOE4* carrier status and visual acuity were adjusted in analysis.

Abbreviation: mfERG, multifocal electroretinography; Aβ, amyloid-β; CN, cognitively normal older adults; Aβ+CN, amyloid positive CN; Aβ-CN, amyloid negative CN

eTable 6. Partial correlation analysis between regional macular thickness and AD-CT in CN individuals.

Regional Macular Thickness	***r***	***p***
Central fovea	0.20	.19
Inner ring average (Parafovea)	0.15	.33
Outer ring average (Perifovea)	0.2	.18

NOTE. Covariates including age, sex, *APOE4* carrier status and visual acuity were adjusted in analysis.

Abbreviations: AD-CT, Alzheimer's disease-signature cortical thickness; CN, cognitively normal

eTable 7. Partial correlation analysis between functional parameters of retina measured by mfERG and AD-CT in CN individuals.

	Amplitude		Implicit time	
Rings	***r***	***p***	***r***	***p***
Ring 1	0.01	.93	0.03	.85
Ring 2	0.23	.14	0.04	.79
Ring 3	0.27	.08	0.08	.61
Ring 4	0.32	.03	0.05	.74
Ring 5	0.32	.03	0.08	.61
Ring 6	0.29	.06	0.01	.93

NOTE. Covariates including age, sex, *APOE4* carrier status and visual acuity were adjusted in analysis.

Abbreviations: AD-CT, Alzheimer's disease-signature cortical thickness; CN, cognitively normal

eFigure 1. Histogram of global [^{11}C] PiB retention (SUVR), a continuous variable, indicating global Aβ deposition in all CN older adults in this study.

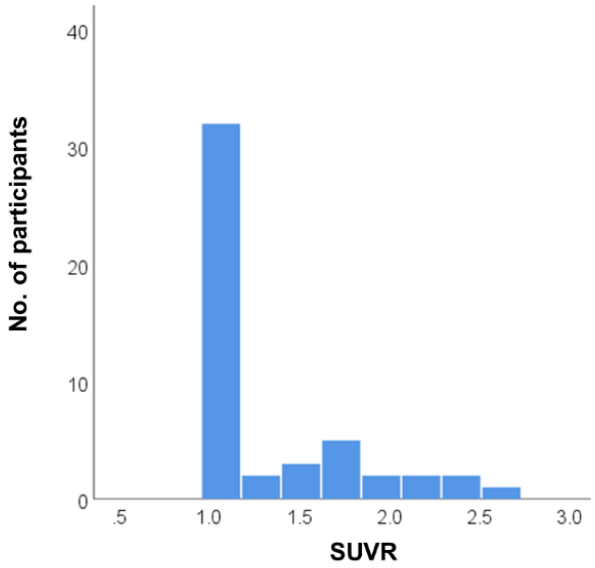

Abbreviation: PiB, Pittsburgh Compound-B; SUVR, standardized uptake value ratio; Aβ, beta-amyloid; CN, cognitively normal

eFigure 2. Subregional analyses of the correlations between Alzheimer disease-signature cortical thickness (AD-CT) and ganglion cell-inner plexiform layer thickness (GCIPL-T). A Pearson correlation coefficient and p-value of partial correlation analysis between AD-CT and GCIPL-T in each subfiled are presented.

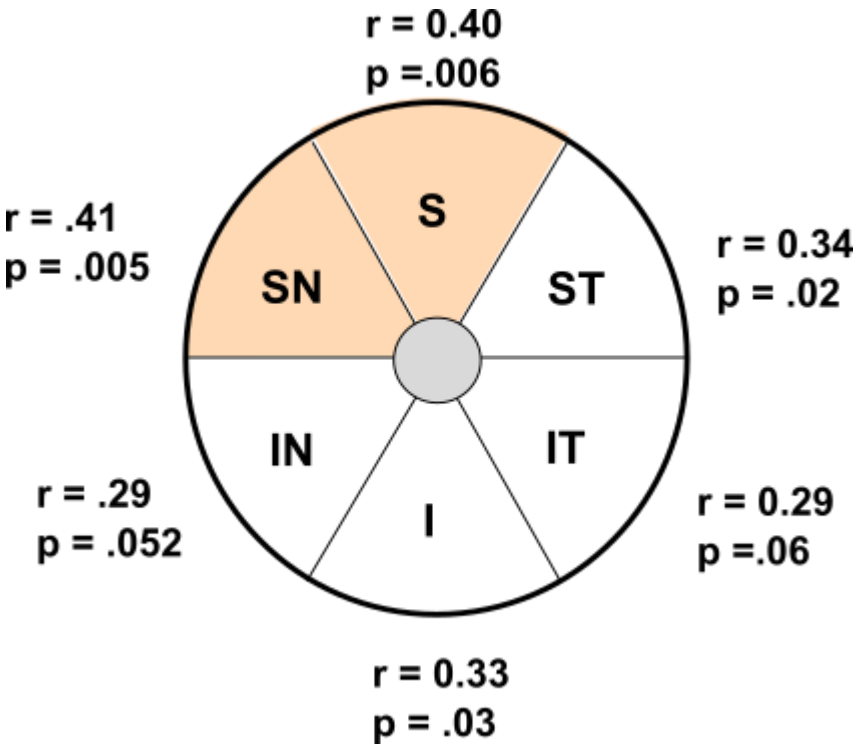

Abbreviation: SN, superonasal; ST, superotemporal; IN, inferonasal; IT, inferotemporal; T, temporal; S, superior; I, inferior

eFigure 3. Receiver operating characteristic (ROC) curve analysis of the model to detect CN older adults with preclinical AD using retinal imaging biomarkers. A green line indicates the final model selected from multivariate logistic regression analyses using backward likelihood method, which included thickness in the inner nasal subfield of the macula and the retinal nerve fiber layer (RNFL) thickness in the inferior quadrant after adjusting fixed variables (*i.e.*, age, sex, APOE4, and best corrected visual acuity), while a gray line indicates the reference model including only fixed variables.

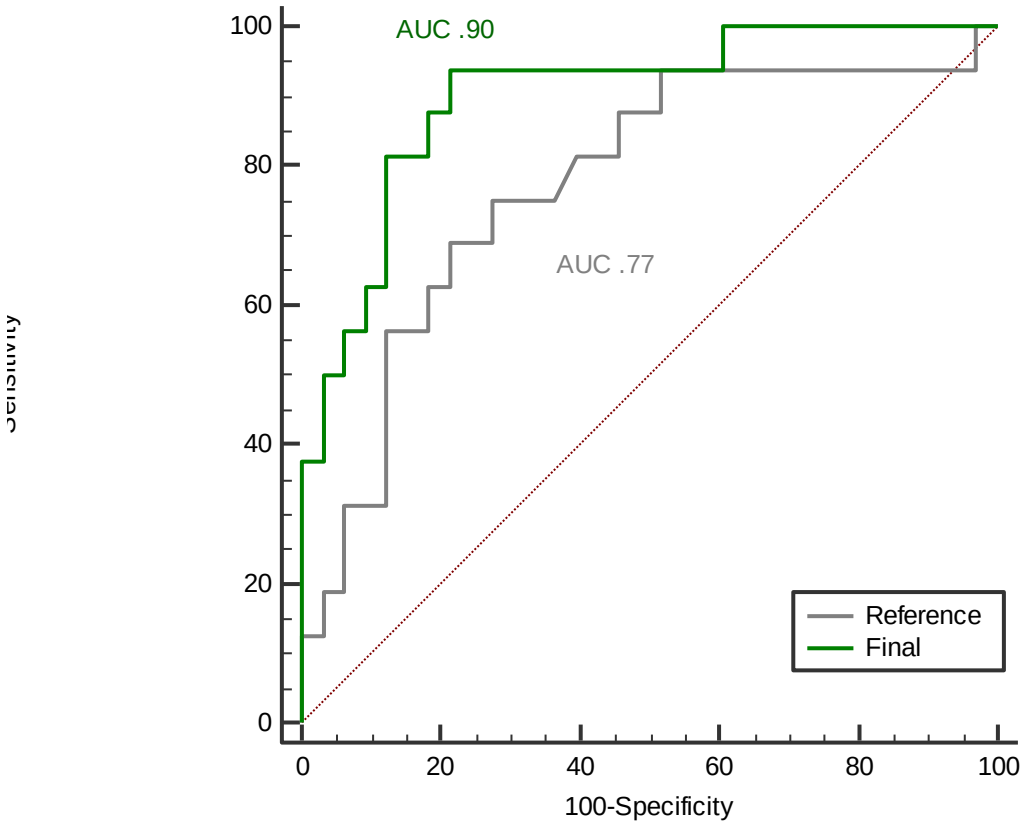

eReferences

1. Byun MS, Yi D, Lee JH, et al. Korean Brain Aging Study for the Early Diagnosis and Prediction of Alzheimer's Disease: Methodology and Baseline Sample Characteristics. *Psychiatry Investig.* 2017;14(6):851-863.

2. Lee JH, Lee KU, Lee DY, et al. Development of the Korean version of the Consortium to Establish a Registry for Alzheimer's Disease Assessment Packet (CERAD-K): clinical and neuropsychological assessment batteries. *J Gerontol B Psychol Sci Soc Sci.* 2002;57(1):P47-53.

3. Lee DY, Lee KU, Lee JH, et al. A normative study of the CERAD neuropsychological assessment battery in the Korean elderly. *J Int Neuropsychol Soc.* 2004;10(1):72-81.

4. Wenham PR, Price WH, Blandell G. Apolipoprotein E genotyping by one-stage PCR. *Lancet.* 1991;337(8750):1158-1159.

5. Byun MS, Kim HJ, Yi D, et al. Differential effects of blood insulin and HbA1c on cerebral amyloid burden and neurodegeneration in nondiabetic cognitively normal older adults. *Neurobiol Aging.* 2017;59:15-21.

6. Tzourio-Mazoyer N, Landeau B, Papathanassiou D, et al. Automated anatomical labeling of activations in SPM using a macroscopic anatomical parcellation of the MNI MRI single-subject brain. *Neuroimage.* 2002;15(1):273-289.

7. Reiman EM, Chen K, Liu X, et al. Fibrillar amyloid-beta burden in cognitively normal people at 3 levels of genetic risk for Alzheimer's disease. *Proc Natl Acad Sci U S A.* 2009;106(16):6820-6825.

8. Villain N, Chetelat G, Grassiot B, et al. Regional dynamics of amyloid-beta deposition in healthy elderly, mild cognitive impairment and Alzheimer's disease: a voxelwise PiB-PET longitudinal study. *Brain.* 2012;135(Pt 7):2126-2139.

9. Chetelat G, La Joie R, Villain N, et al. Amyloid imaging in cognitively normal individuals, at-risk populations and preclinical Alzheimer's disease. *Neuroimage Clin.* 2013;2:356-365.

10. Jack CR, Jr., Wiste HJ, Weigand SD, et al. Age-specific population frequencies of cerebral beta-amyloidosis and neurodegeneration among people with normal cognitive function aged 50-89 years: a cross-sectional study. *Lancet Neurol.* 2014;13(10):997-1005.

11. Jack CR, Jr., Wiste HJ, Weigand SD, et al. Different definitions of neurodegeneration produce similar amyloid/neurodegeneration biomarker group findings. *Brain.* 2015;138(Pt 12):3747-3759.

12. Aizenstein HJ, Nebes RD, Saxton JA, et al. Frequent amyloid deposition without significant cognitive impairment among the elderly. *Arch Neurol.* 2008;65(11):1509-1517.

13. Cohen AD, Mowrey W, Weissfeld LA, et al. Classification of amyloid-positivity in controls: comparison of visual read and quantitative approaches. *Neuroimage.* 2013;71:207-215.

14. Choe YM, Sohn BK, Choi HJ, et al. Association of homocysteine with hippocampal volume independent of cerebral amyloid and vascular burden. *Neurobiol Aging.* 2014;35(7):1519-1525.

15. Park JC, Han SH, Yi D, et al. Plasma tau/amyloid-beta1-42 ratio predicts brain tau deposition and neurodegeneration in Alzheimer's disease. *Brain.* 2019;142(3):771-786.

16. Fantoni E, Collij L, Lopes Alves I, Buckley C, Farrar G, consortium A. The Spatial-Temporal Ordering of Amyloid Pathology and Opportunities for PET Imaging. *J Nucl Med.* 2020;61(2):166-171.

17. Hood DC, Bach M, Brigell M, et al. ISCEV guidelines for clinical multifocal electroretinography (2007 edition). *Doc Ophthalmol.* 2008;116(1):1-11.

18. DeLong ER, DeLong DM, Clarke-Pearson DL. Comparing the areas under two or more correlated receiver operating characteristic curves: a nonparametric approach. *Biometrics.* 1988;44(3):837-845.

